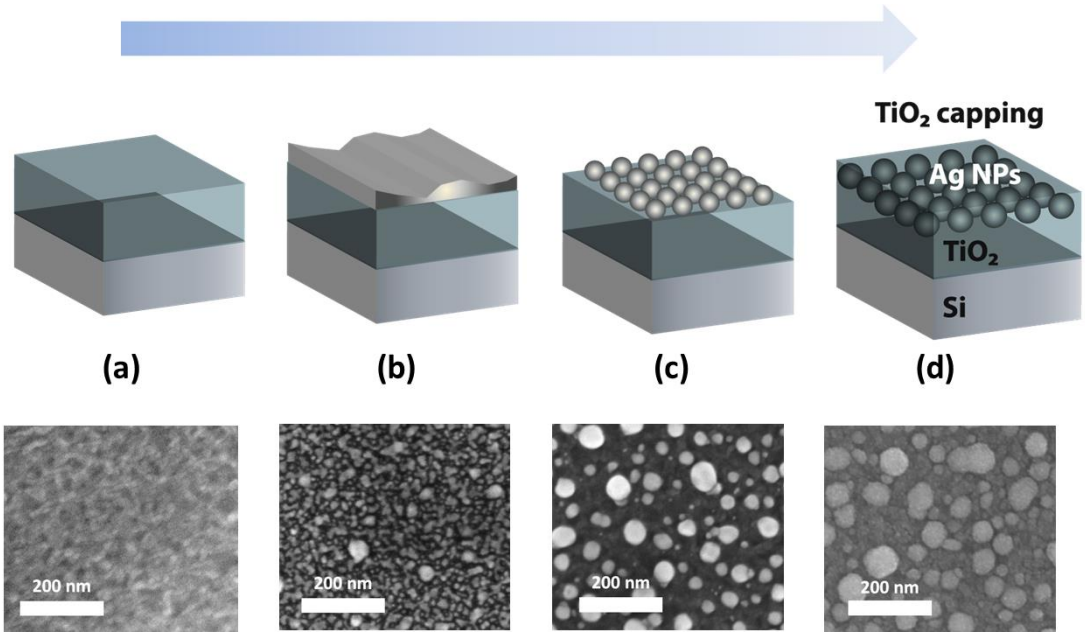

From left to right, schematic representation and Scanning Electron Microscopy images of the nanocomposite at each step of the elaboration process: (a) TiO_2 substrate deposition, (b) Ag (5 nm) deposition and (c) nanostructuration via thermal annealing (at 400°C for 1 h), and (d) deposition of a TiO_2 capping layer.

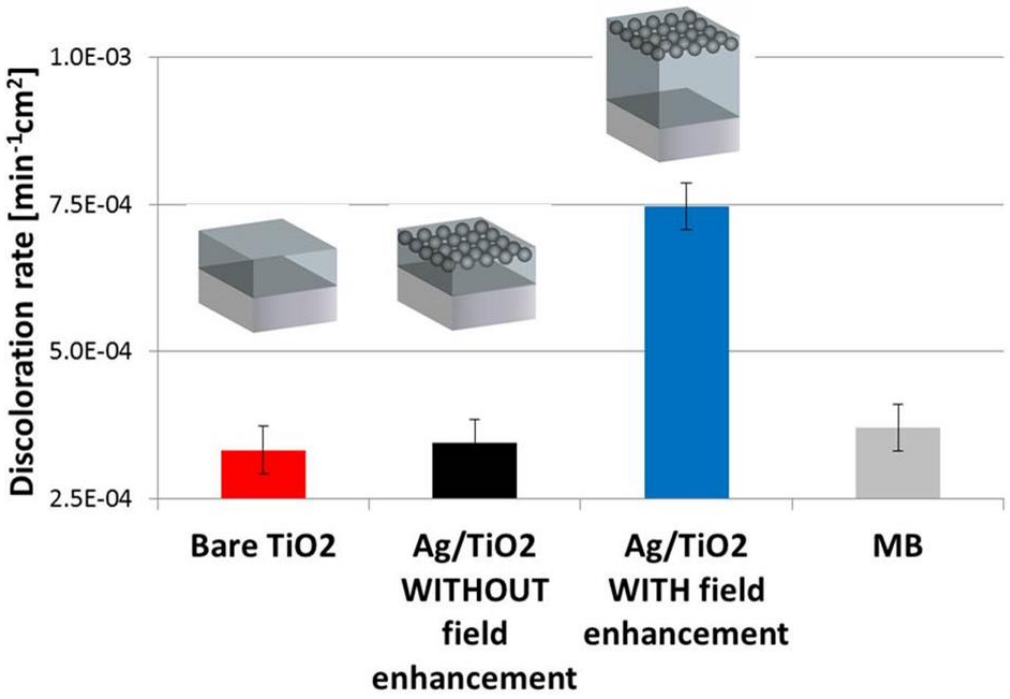

Discoloration test results under visible irradiation. As expected, TiO_2 is not active under visible illumination. Despite having the same composition and superficial morphology,

the two TiO_2/Ag/TiO_2 nanocomposite film showed completely different behavior. In particular, the film matching the plasmonic field enhancement conditions is able to decompose the MB dye.

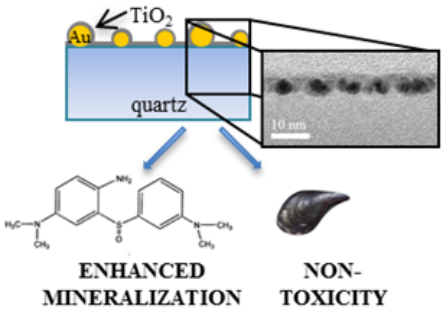

TiO2 wrapping of Au nanoparticles for eco-friendly water/wastewater purification.

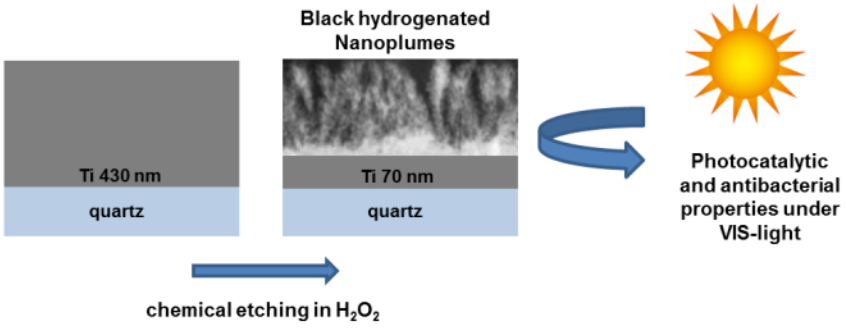

Photoactive hydrogenated TiO2 nanoplumes with photocatalytic and antibacterial properties under VIS-light.

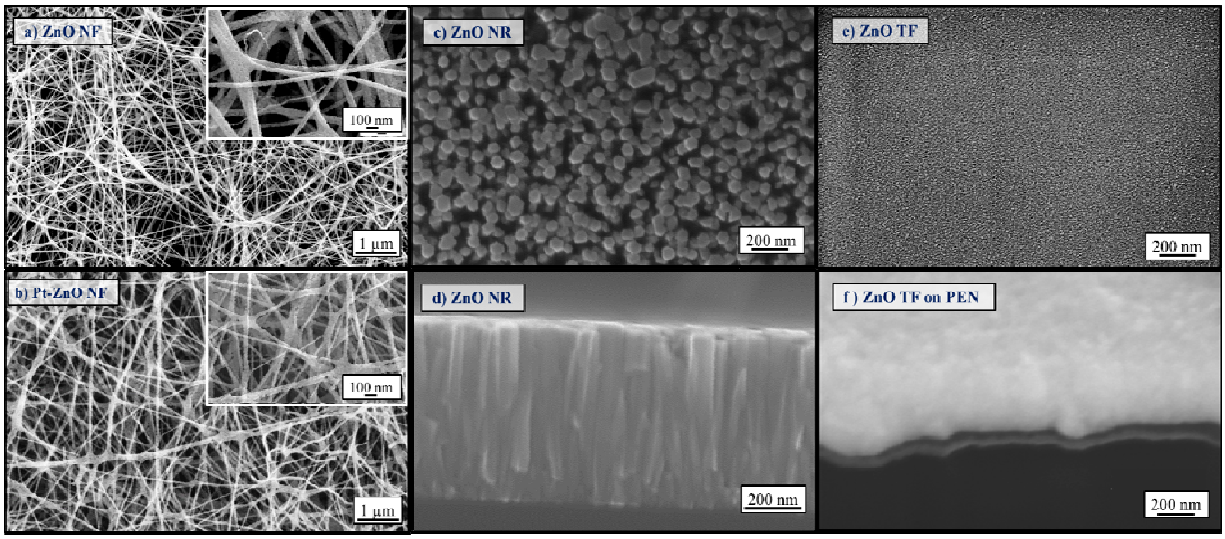

SEM images of ZnO NF (a) and Pt-ZnO NF (b) (inset: higher magnification images); ZnO NRs grown on 3 nm thin film deposited by ALD: plan view of ZnO NRs grown (c) and cross section (d); ZnO TF plan view on Silicon (e) and cross section on PEN (f).

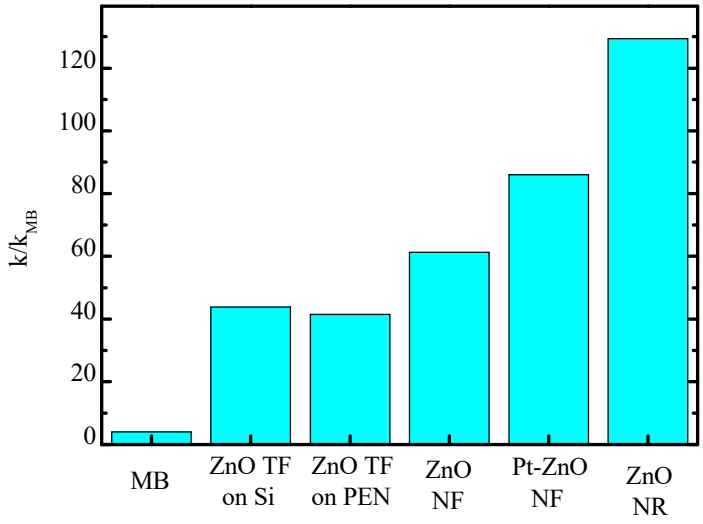

Photo-degradation reaction rate, normalized to the value obtained for the MB in the absence of the catalyst (MB) and for the different investigated samples: ZnO thin film on Silicon (ZnO TF on Si) and on PEN (ZnO TF on PEN), ZnO and Pt-ZnO nanofibers (ZnO NF and Pt-ZnO NF) and ZnO nanorods (ZnO NR) onto 3 thin films.

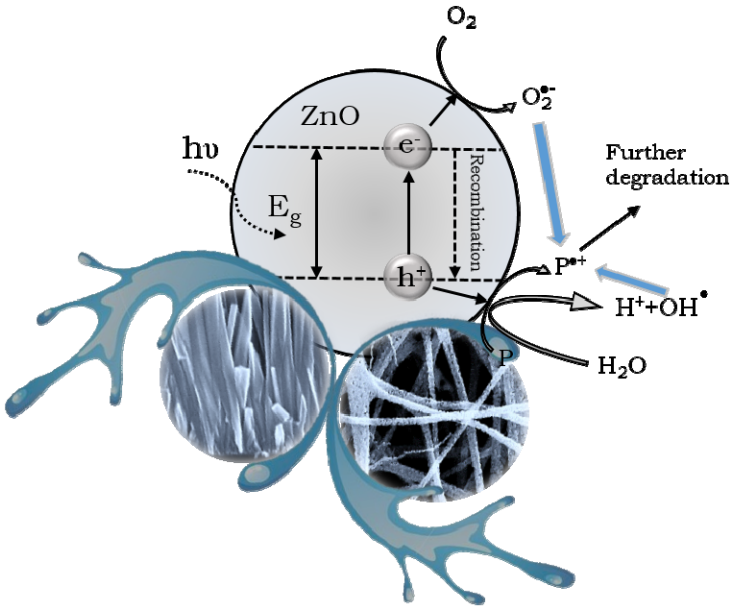

The photocatalytic process of ZnO nanorods and nanofibers.

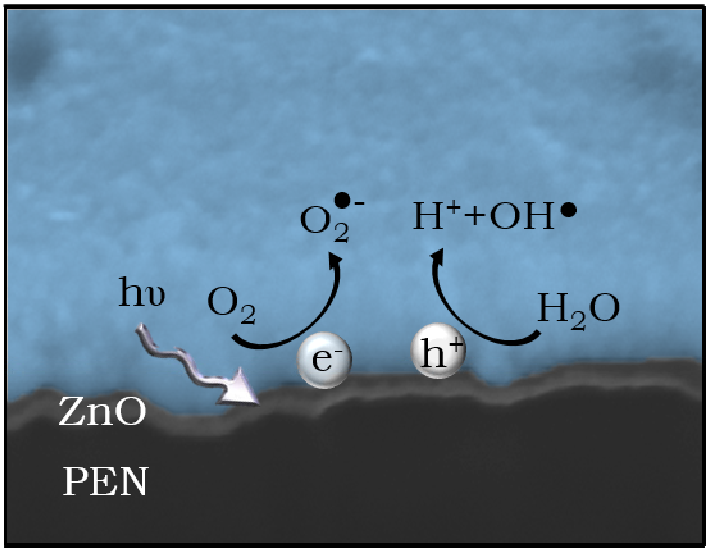

The photocatalytic process of ZnO thin film on polyethylene naphtalate.

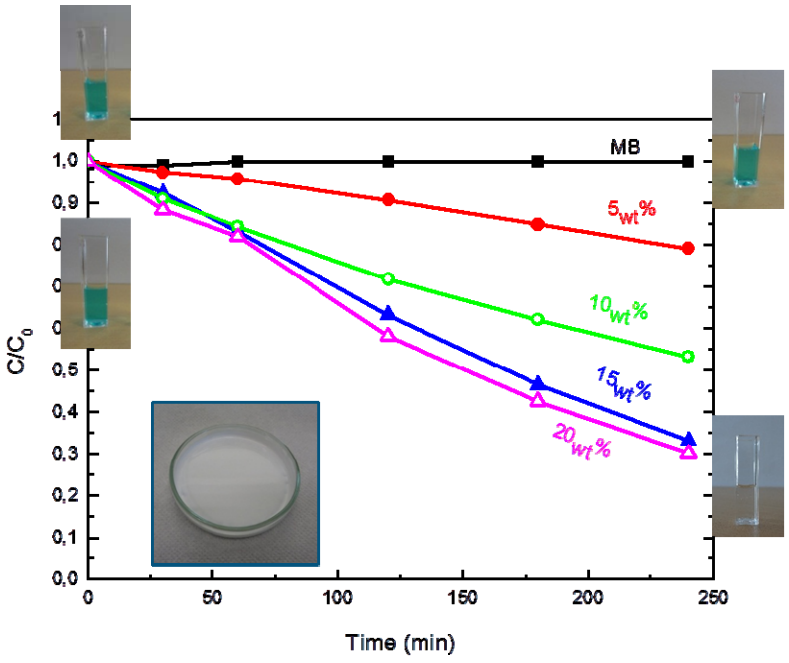

Photocatalytic activity of PMMA/TiO_2 films with 5_{wt}% NPs (full dots), with 10_{wt}% NPs (open dots), with 15_{wt}% NPs (full triangles) and with 20_{wt}% NPs (open triangles) compared to the discoloration of pure MB under UV illumination (squares). Inset: PMMA/TiO_2 films with 15_{wt}% NPs in the Petri dish.

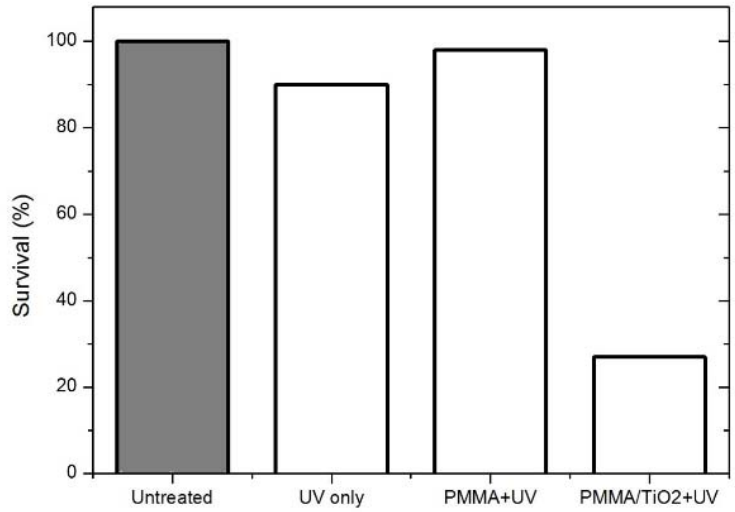

E. coli survival rate for CFU count after 60 min exposure to 1 cm^2 $PMMA/TiO_2$ film with 15_{wt}% NPs and to PMMA film. Untreated control and UV control were run in parallel.

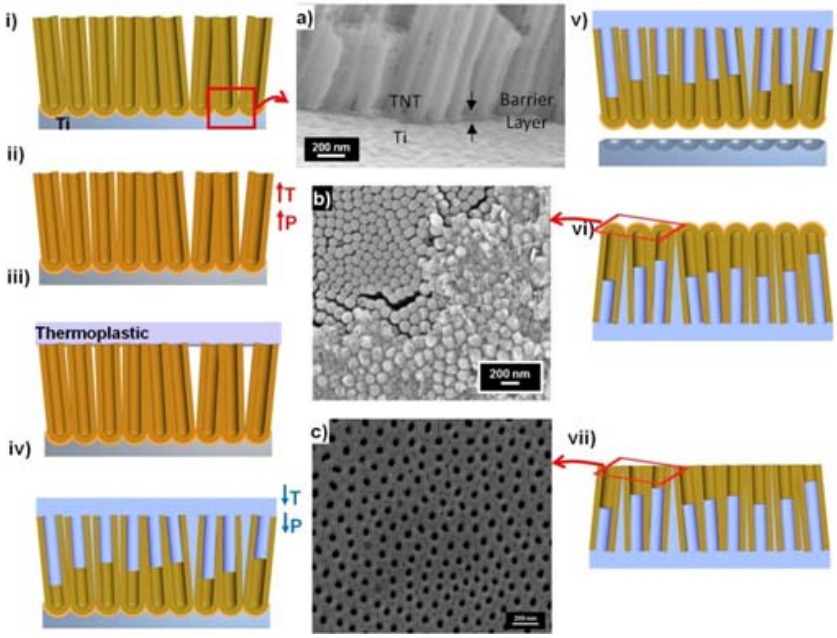

i) Initial annealed TNT. a) Cross-section view of TNT with the barrier layer. ii) Increasing of temperature with associated increasing of pressure. iii) TP layer on the top of TNT iv) Decreasing of temperature and pressure and fast infiltration of the TP into the TNT and cracks. v) Peeling-off of the TNT/TP from the Ti. b) Detailed view of the as-obtained nanocomposite with some areas covered with the barrier layer and thermal TiO2. vii) Permeation process c) Surface of the composite (9 µm TNT, 450 °C, PP) after the permeation process.

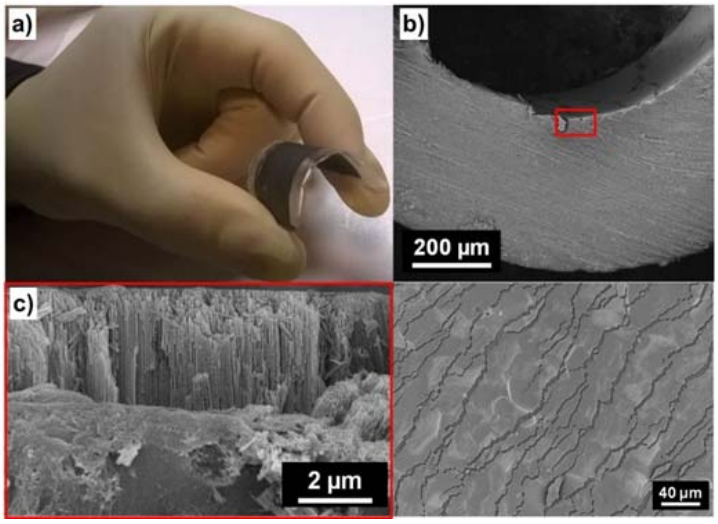

a) Flexible capacities of nanocomposites (12 µm, 600 °C TNT PET). b) Low magnification images of thermoformed nanocomposites (4.5 µm, 600 °C TNT PC). c) High magnification images of b), TNT are on the internal curvature zone. d) Low magnification image of the surface of TNT on the external curvature zone.

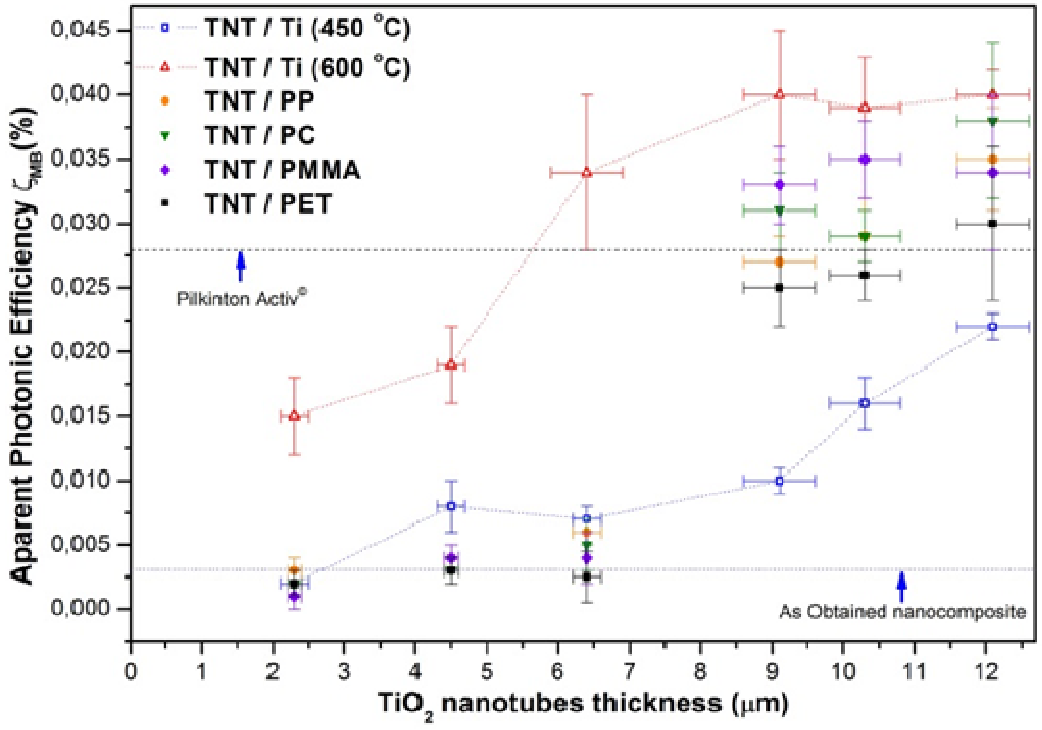

Photonic efficiency of TNT on Ti annealed at 450 and 600°C and nanocomposites with TNT annealed at 600°C, as a function of TNT thickness. Reported PE of commercial product (Pilkinton Active ©) and as obtained nanocomposites are included as dotted lines, note the blue arrows, for comparison. Lines for TNT on Ti are only for eye guiding.

	Control (No UV-A)	Control	TP	**TNT on Ti**	**TNT/TP**
Bacteria survival (%)	80 ± 5	85 ± 10	107 ± 6	**57 ± 6**	**60 ± 5**

Bacterial survival results under UV-A illumination for TNT on Ti and TNT/TP samples containing 600 °C annealed, 9 μm thick TNT. Please note the similar values obtained for TNT on Ti and TNT/TP composites.

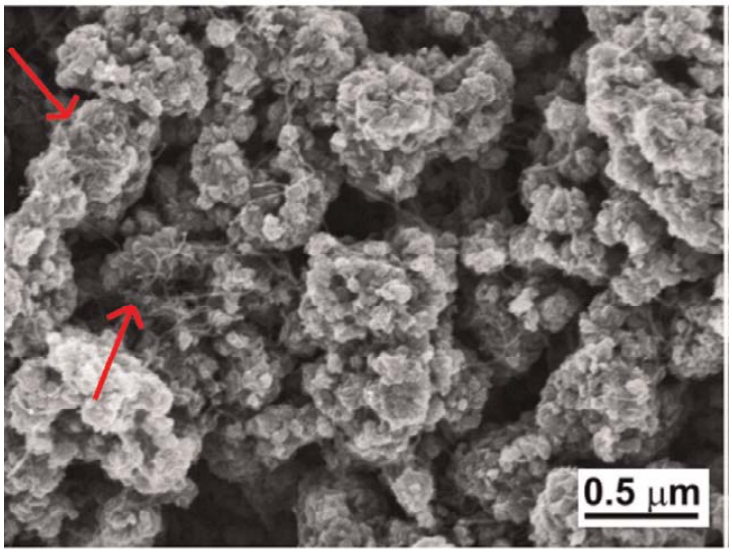

SEM image of the MWCNT-TiO_2 composite layer deposited by electrophoresis on a Pt/SiO_2/Si substrate

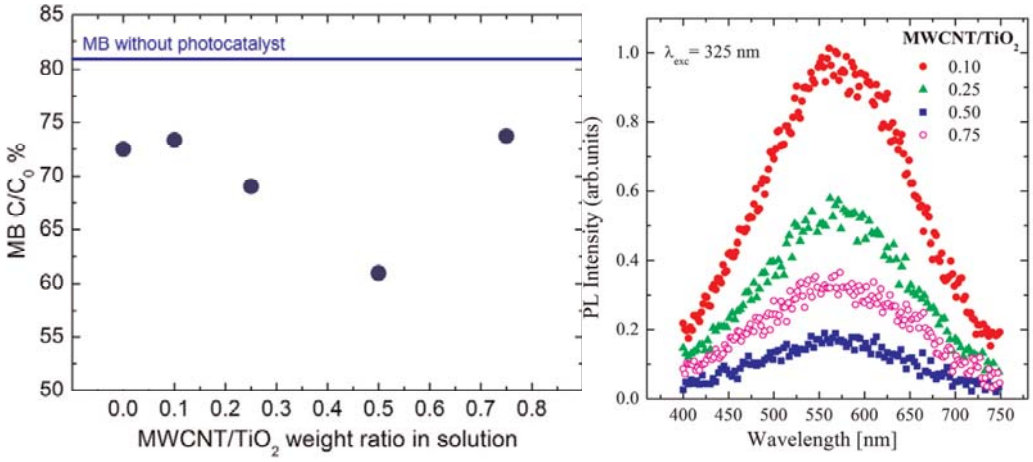

(a) Residual percentage of the initial MB concentration (C_0) calculated from the 664 nm absorbance peak for different MWCNT/np-TiO_2 composites. The blue line shows the residual C/C_0 value of MB after irradiation without the photocatalytic sample; (b) Photoluminescence spectra of the samples with MWCNT/TiO_2 ratio= 0.10, 0.25, 0.50 and 0.75. The excitation wavelength is 325 nm.

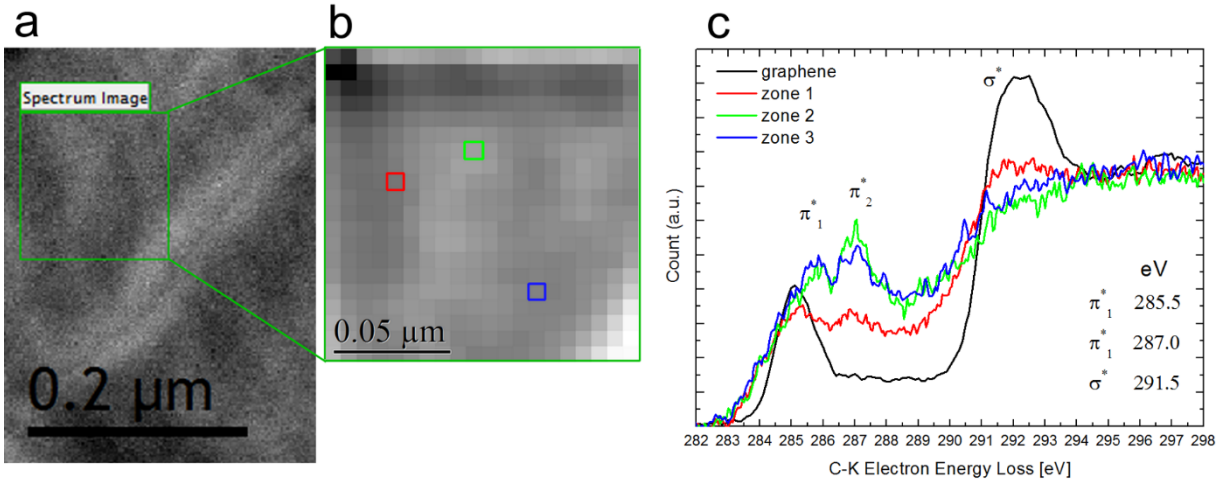

(a) STEM image of Graphene Oxide. The EELS spectrum image was acquired in a selected region (20x20 spectra). The dark field of the detector is reported in (b). The experimental EELS spectra of the C K-edge electron energy loss in three different zones (red, green and blue squares in (b)) are shown on the right (c). The experimental EELS spectrum of graphene is reported for reference.

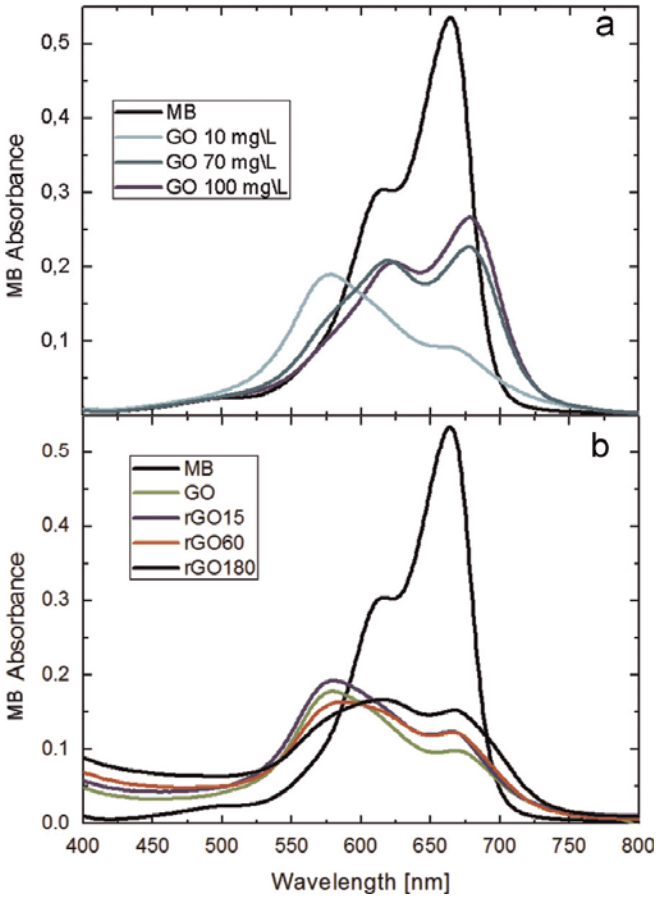

(a) UV–vis absorbance spectra of MB in Graphene Oxide solutions with different concentration values, showing that the formation of dimers/trimers is enhanced at low GO concentration; (b) UV–vis absorbance spectra of MB in GO 10mg/l before and after different laser reduction times (15, 60 and180 min), showing that the formation of dimers/trimers is suppressed as the GO is reduced.

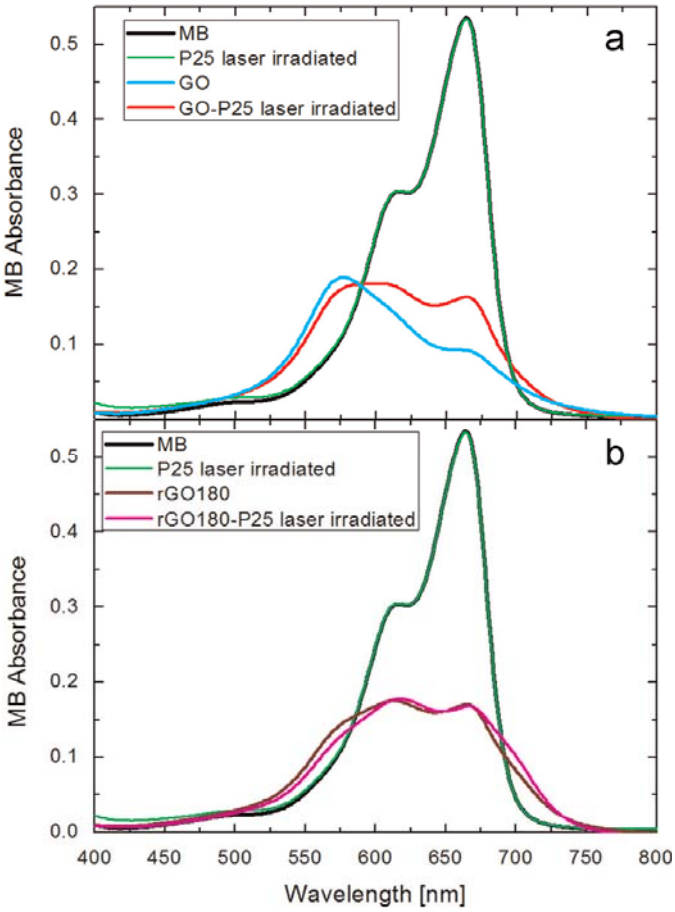

(a) UV–vis absorption spectra of laser irradiated GO–P25 solution compared to 10mg/l GO solution. (b) UV–vis absorption spectra of laser irradiated rGO180– P25 solution compared to 10mg/l rGO180 solution.10 µl of MB for ml of solution were added to all samples. UV–vis absorption spectra of laser irradiated 90mg/l P25 solution is reported in both figures.

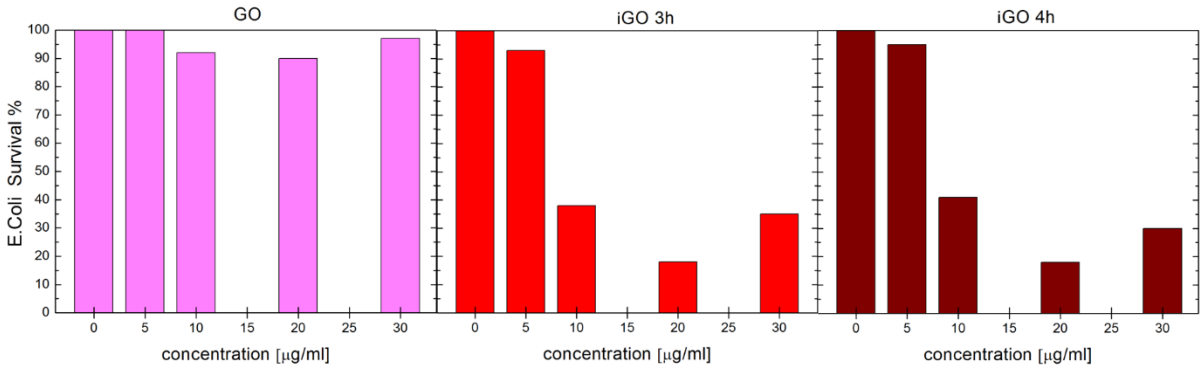

Relative *E. coli* survival rate measured by CFU count after 1h exposure to Graphene Oxide, iGO3 and iGO4 at different final concentrations. Untreated controls were run in parallel. Data were normalized to the untreated sample.

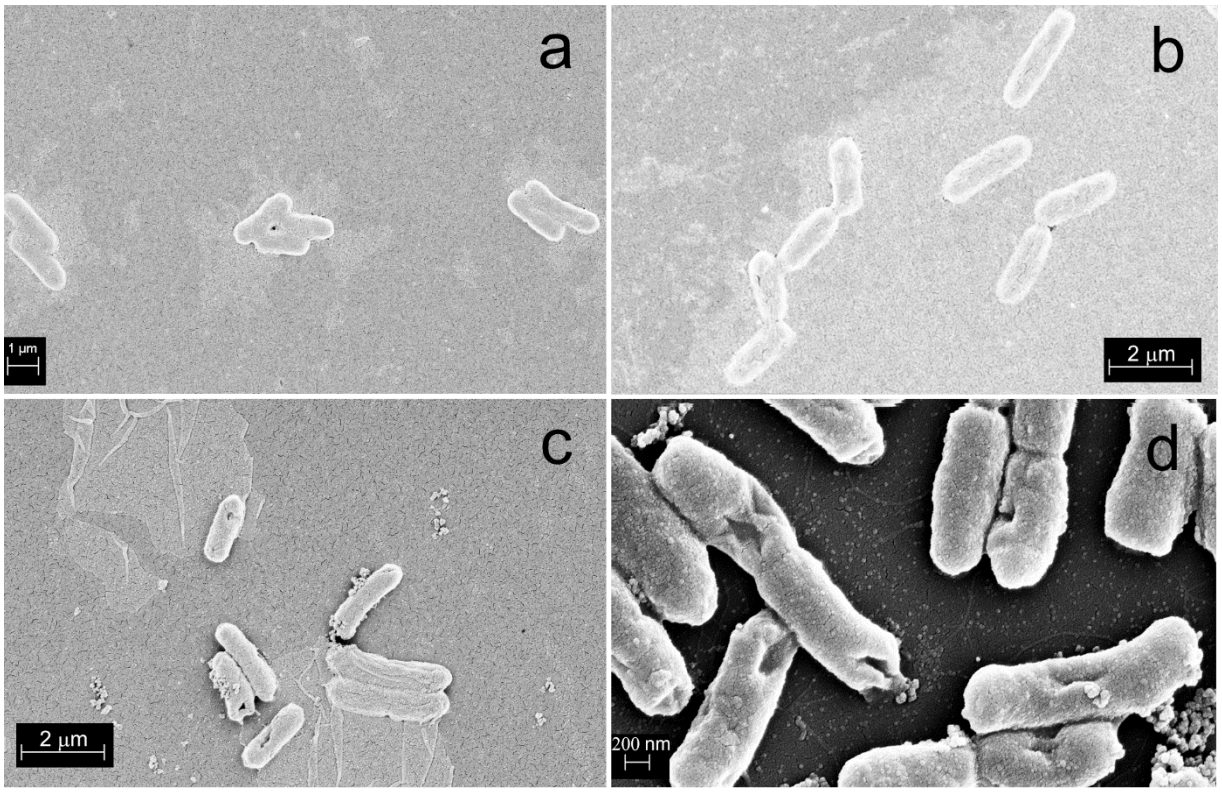

SEM images of untreated E. Coli (a) and of E. Coli after 1 h of exposure to 30 mg/l of GO (b) or to 30 mg/l of iGO3 (c and d). In the latter images bacteria are visibly damaged.

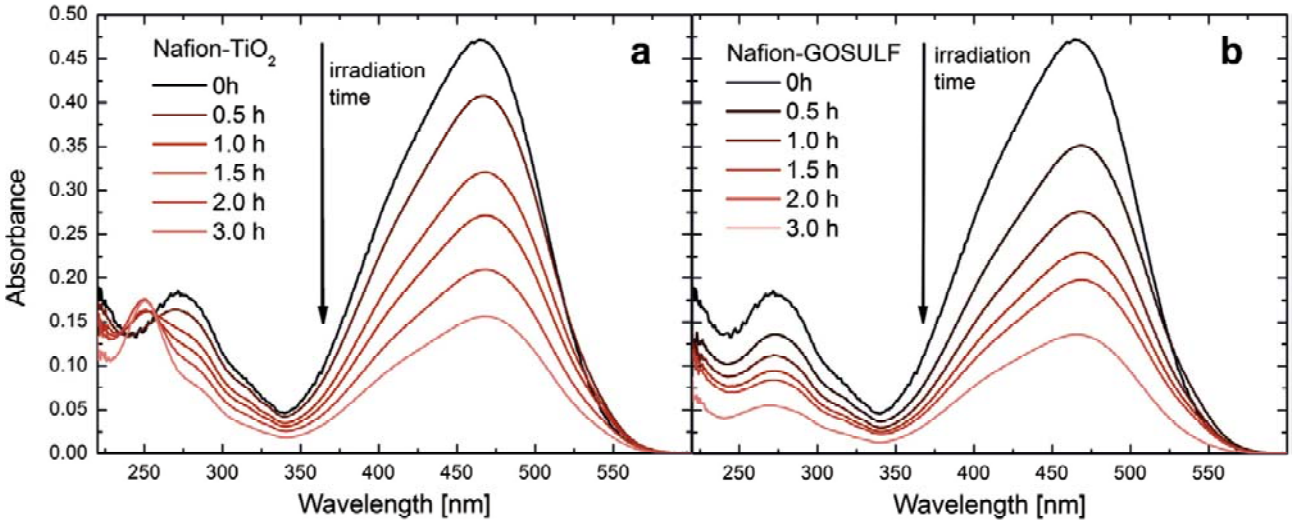

UV–Vis absorbance spectra of MO solution after irradiation for three hours in the presence of Nafion-TiO_2 (a) and Nafion-GO_{SULF} (b). MO degradation by Nafion-TiO_2 shows the formation of possible toxic by-products (aromatic compounds) identified by the peak at 250nm, whereas the MO degradation performed by Nafion-GO_{SULF} does not present the formation of such species.

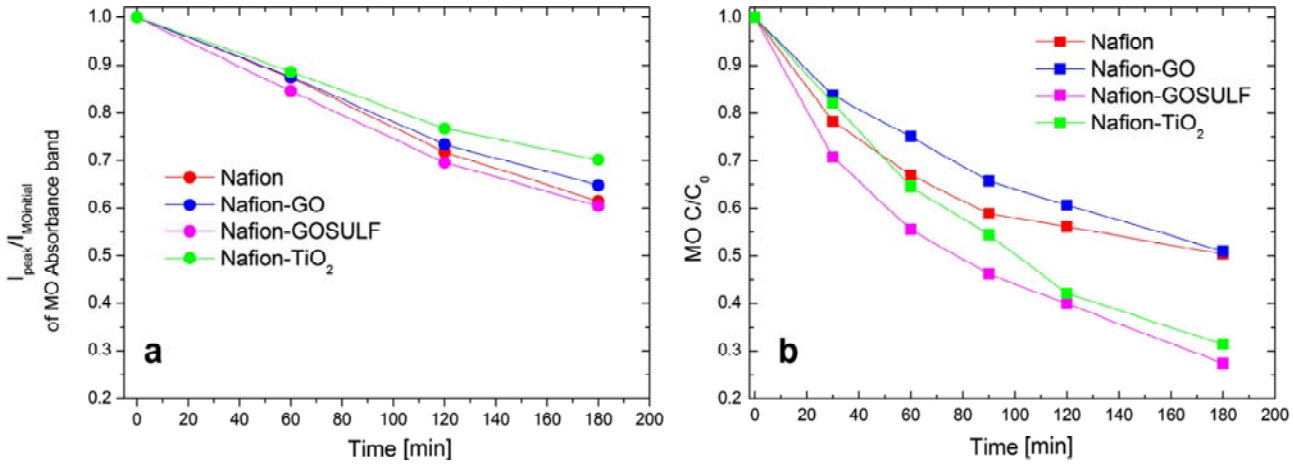

(a) The maximum value of MO absorbance after the adsorption by the different hybrid membranes for different times and (b) the residual MO concentration during the UVA/Vis irradiation time.

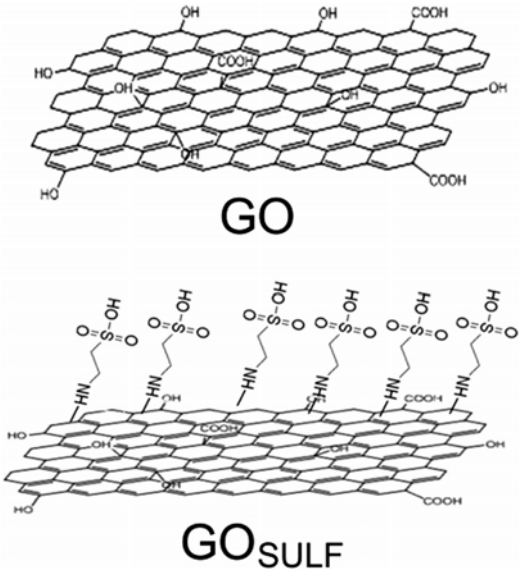

Schematic representation of the structures of Graphene Oxide (top) and GO_{SULF} nanoplatelets (bottom).

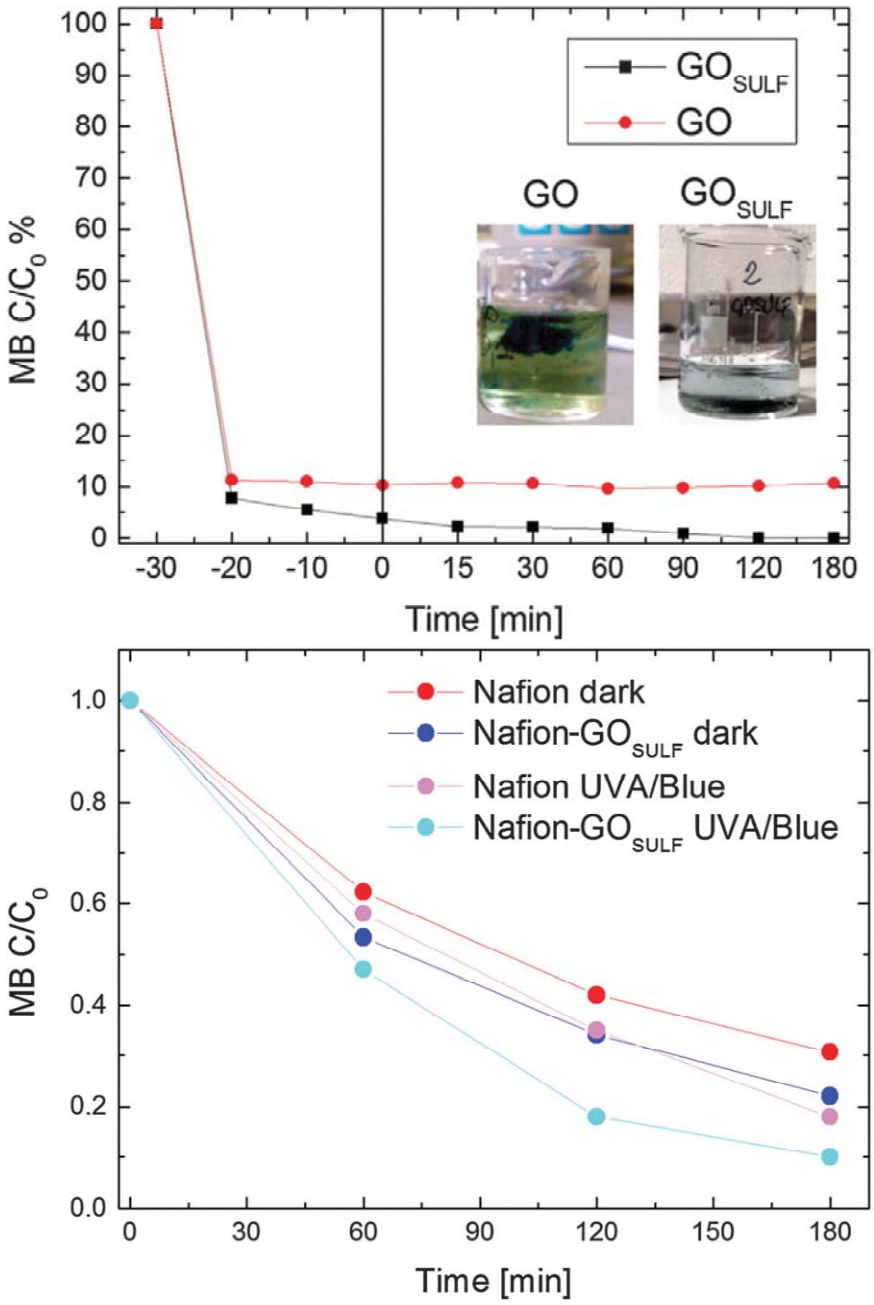

(a) MB residual concentration versus time of contact with GO and GO_{SULF} powders (both with a concentration of 70 mg/l). The UV-blue lamp irradiation starts after 30 min of adsorption in the dark, as indicated by the vertical line at t = 0 min. Lines in the figure are guide to the eye. The photos in the inset show the beakers containing the MB solutions with GO_{SULF} and GO after 10 min adsorption (t = -20); (b) MB residual concentration versus time of contact with Nafion and Nafion–GO_{SULF} in the dark (red and blue dots, respectively) and under irradiation (magenta and cyan dots, respectively).

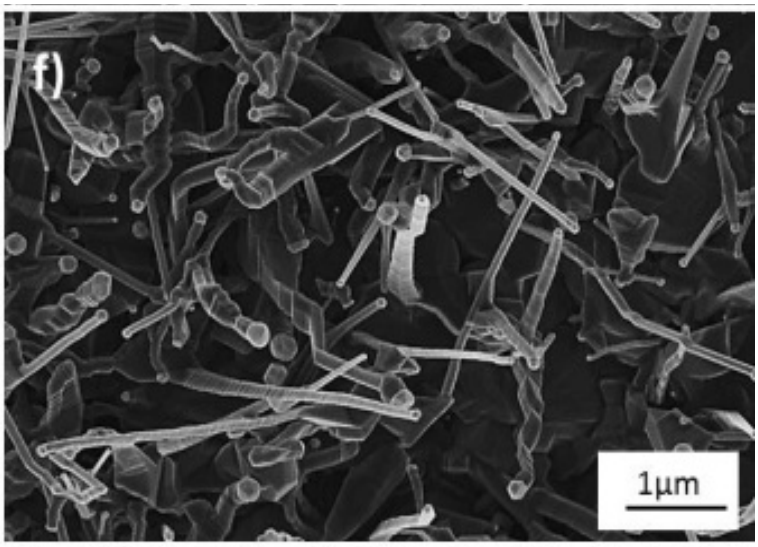

SEM plan view of TiO_2 NWs synthetized by seed assisted thermal growth at the optimal conditions: 800°C, 4h, 7.5 lpm of O_2 and 10 lpm of Ar.

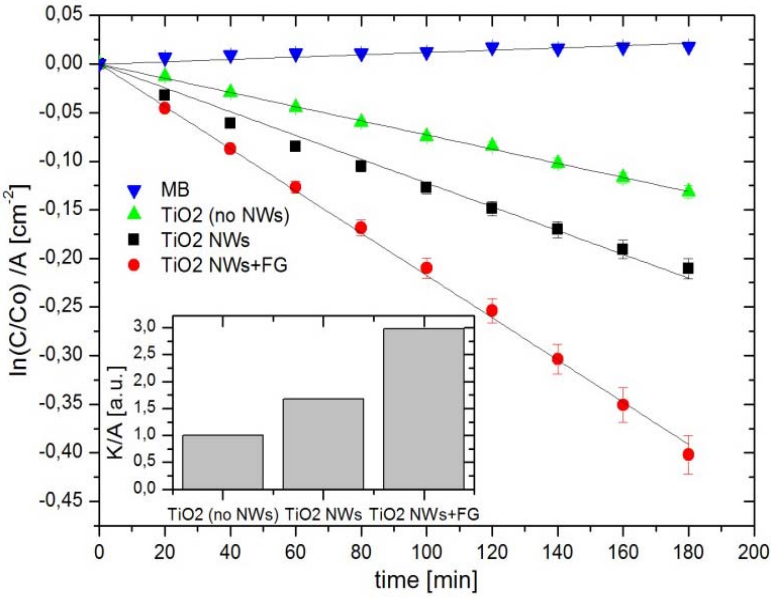

Photocatalytic activity of various samples: MB reference solution without any TiO_2 sample (blue downward triangles); TiO_2 reference foil without NWs (green upward triangles); TiO_2 foil with NWs (black squares); TiO_2 foil with NWs and additional annealing in forming gas (FG, red circles). Inset: degradation rate per unit area (K/A) of the samples normalised to the K/A obtained from the TiO_2 reference foil without NWs.

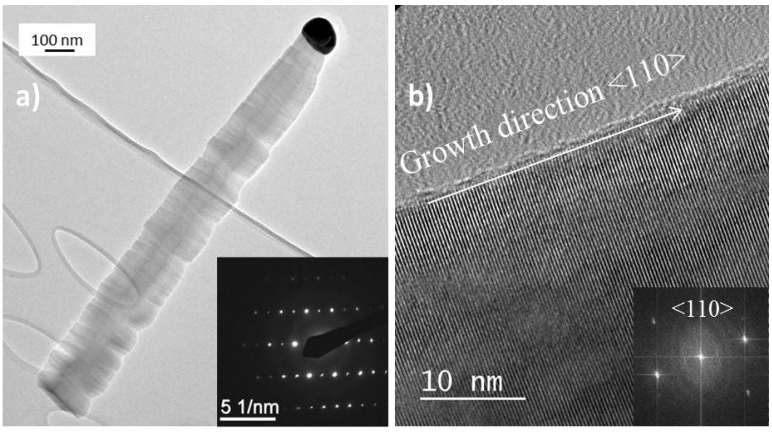

a) TEM image of a single NW and its diffraction pattern (inset) showing that it is a single crystal; b) High resolution TEM of the NW and the corresponding Fast Fourier Transform (inset) revealing its growth direction.

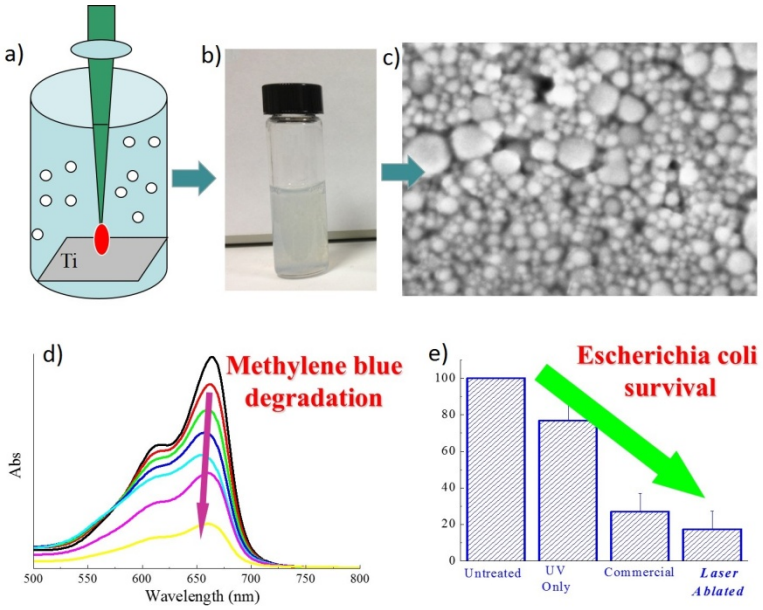

a) A scheme of the laser ablation process: a pulsed high energy laser beam was focused on a surface of a Ti target immersed in pure water. TiO_2 Nanoparticles form in solution. b) A photo of a typical TiO_2 nanoparticles colloidal solution. c) High resolution scanning electron image of nanoparticles obtained by pulsed laser ablation in liquid process. d) Photodegradation test. Absorbance spectra of Metilene Blue dye (MB) for different UV irradiation time. Photodegradation of the dye is due to the catalytic action of TiO_2Nps under UV illumination. e) Antibacterial activity test. Relative *E. coli* survival rate obtained through “CFU count” after 60’ exposition to TiO_2 Nps and UV radiation. Untreated control (Untreated), UV control (UV only) and commercial nanoparticles (Commercial) were run in parallel.

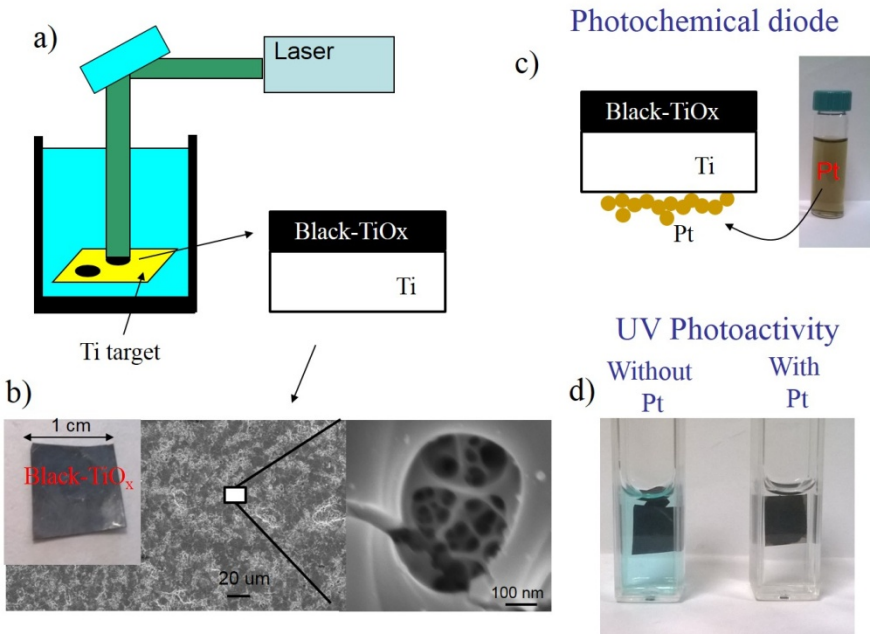

a) A scheme of the laser ablation process: a pulsed high energy laser beam impinge on a surface of a Ti target immersed in pure water with the formation of a “Black-TiOx” material. b) (left) Photo of a 1 cm x 1 cm Ti foil uniformly irradiated. (centre and right) Scanning electron images of surface of the Ti foil after irradiation. The black irradiated surface is uniformly covered by cavities of several hundreds of nm in diameter with inside a branched porous nano-structure. c) Scheme of the photochemical diode realized with black-TiOx and Pt nanoparticles sandwiched together. d) Photo-decolouration test. Photo of methylene blue dye solutions treated with the developed “photochemical diode”. Sample without (left) and with (right) platinum deposition shows a different activity in the decolouration of MB solution. Photo-degradation of the dye is due to the catalytic action of black TiOx under UV illumination. Photo are taken after 12 hour of UV irradiation.

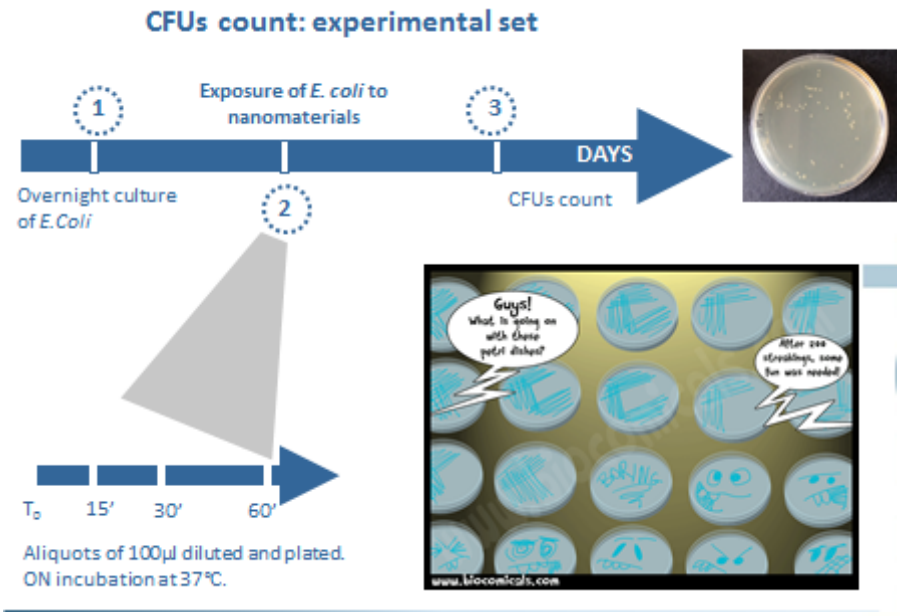

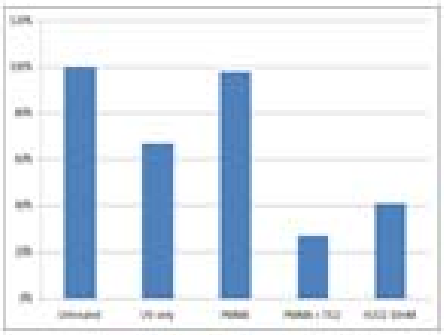

PMMA + TiO_2

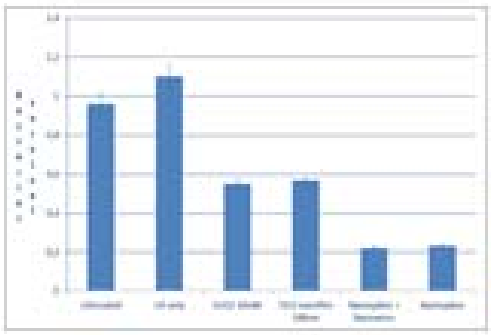

TiO_2 thermally grown nanospikes

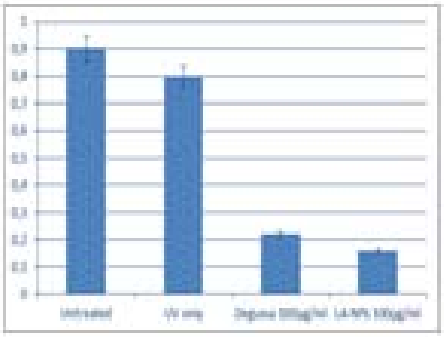

TiO_2 LA-NPs

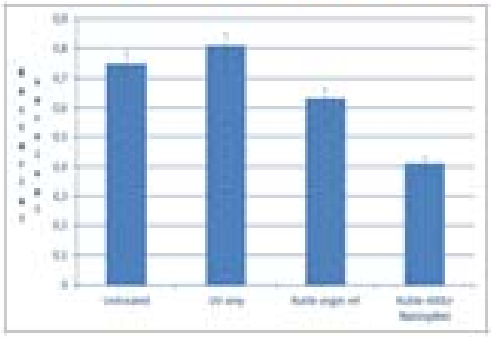

TiO_2 Flat rutile vs nanospikes

Antibacterial activity tests. On the left: scheme of the CFUs count procedure. On the right: some of the results obtained. On the y axes the percentage of bacterial survival after 60' exposure is shown. Results are normalized toward the untreated sample. The initial bacterial concentration is 10^6 CFUs.

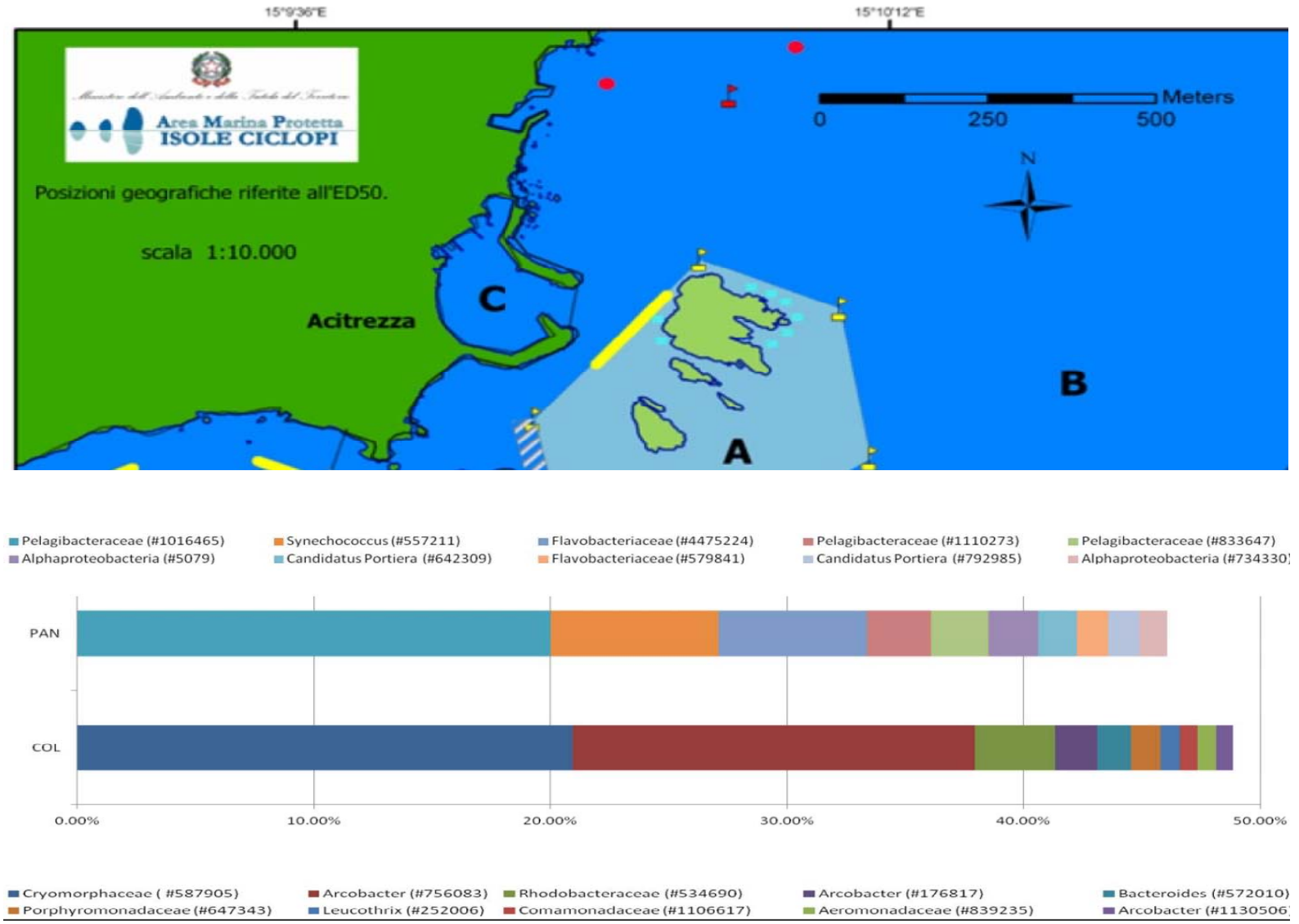

Metagenomics: paving the way for marine microbial ecosystem analysis. Analysis of marine microbial ecosystems. Environmental samples collection points are indicated by the red spots in the map. Results of the core microbiome composition are indicated below the map.